Chemical Kinetic Study of the Effect of a Biofuel Additive on Jet-A1 Combustion†

Philippe Dagaut* and Sandro Gaïl

Centre National de la Recherche Scientifique 1C, Avenue de la Recherche Scientifique, 45071 Orléans Cedex 2, France

Received: November 14, 2006; In Final Form: December 15, 2006

The kinetics of oxidation of kerosene Jet A-1 and a kerosene/rapeseed oil methyl ester (RME) mixture (80/20, mol/mol) (biokerosene) was studied experimentally in a jet-stirred reactor at 10 atm and constant residence time, over the temperature range 740−1200 K, and for variable equivalence ratios (0.5−1.5). Concentration profiles of the reactants, stable intermediates, and final products were obtained by probe sampling followed by on-line and off-line gas chromatography analyses. The oxidation of these fuels in these conditions was modeled using a detailed kinetic reaction mechanism consisting of 2027 reversible reactions and 263 species. The surrogate biokerosene model fuel used here consisted of a mixture of *n*-hexadecane, *n*-propylcyclohexane, *n*-propylbenzene, and *n*-decane, where the long-chain methyl ester fraction was simply represented by *n*-hexadecane. The proposed kinetic reaction mechanism used in the modeling yielded a good representation of the kinetics of oxidation of kerosene and biokerosene under jet-stirred reactor conditions and of kerosene in a premixed flame. The data and the model showed the biokerosene (Jet A-1/RME mixture) has a slightly higher reactivity than Jet A-1, whereas no major modification of the product distribution was observed besides the formation of small unsaturated methyl esters produced from RME's oxidation. The model predicts no difference in the ignition delays of kerosene and biokerosene. Using the proposed kinetic scheme, the formation of potential soot precursors was studied with particular attention.

Introduction

Environmental concerns about global warming and air pollution are growing. Also, the gap between the growth rate of oil production and demand is increasing. Therefore, sustainable and environmentally friendly fuels are needed for the future. Biofuels derived from vegetable oils may be considered sustainable if sufficient quantities of plants can be grown. Furthermore, this can be viewed as a step toward a "carbon neutral" fuel economy. Biofuels could be mixed in small quantities (5−20%) with current kerosene[1−3] as is already done with biodiesel.[4] Biodiesel is a mixture of monoalkyl esters of long-carbon-chain fatty acids obtained from renewable lipid feedstock (vegetable, animal, waste). Alkyl esters from vegetable oils or animal fat are obtained by transesterification with mostly methanol, but also ethanol:

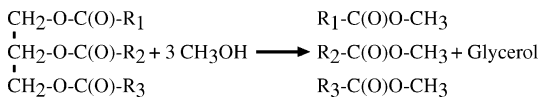

The alkyl esters made from different vegetable oils or animal fat have already been successfully tested in conventional diesel engines as well as in direct-injection engines.[4−12] The reported reduced emissions of carbon oxides and polyaromatic hydrocarbons (PAHs) make biodiesel useful for preserving our environment.[4−8]

Rapeseed oil methyl esters (RMEs) derive from one of the main crops growing in Europe. RME is a complex mixture of C_{14}−C_{22} esters with a highly saturated carbon chain (ca. 94 wt % mostly monounsaturated esters). A previous kinetic study of RME combustion showed a strong similitude between the oxidation of *n*-hexadecane and that of RME,[13] allowing the use of *n*-hexadecane as a chemical surrogate model fuel for modeling RME kinetics of oxidation.

Kerosene (Jet A, Jet A-1, JP-8, TR0) is a complex mixture of alkanes (50−65 vol %), mono- and polyaromatics (10−20 vol %), and cycloalkanes or naphthenes (mono- and polycyclic, 20−30 vol %). It represents the most important fuel for air transportation, whereas recent research indicated it would be suitable for HCCI engine combustion.[14] The average chemical formula for kerosene (Jet A, Jet A-1, TR0, JP-8) differs from one source to another.[15] As before,[15−17] we adopted the formula $C_{11}H_{22}$. Due to the complex composition of this fuel, it is necessary to use a surrogate model fuel for simulating its oxidation. Under high-pressure jet-stirred reactor (JSR) conditions, the detailed kinetic modeling of kerosene oxidation was initially performed using *n*-decane as a model fuel,[16] since *n*-decane and kerosene showed very similar oxidation rates under JSR[16,17] and premixed flame conditions.[18] It was previously shown[13] that *n*-decane is a reasonable model fuel for modeling kerosene oxidation if the formation of aromatics is not a major issue since the oxidation of *n*-decane yields much less aromatic hydrocarbons than kerosene. Therefore, more complex model fuels are necessary to model the formation of aromatics from the oxidation of kerosene.[19−23] Surrogate model fuels consisting of *n*-decane and mixtures of *n*-decane with simple aromatic hydrocarbons and cycloalkanes were recently tested, showing good kerosene oxidation modeling can be achieved using the three-component model fuel surrogate mixture of *n*-decane, *n*-propylbenzene, and *n*-propylcyclohexane.[23]

In this paper, we present new experimental results obtained in a JSR for the oxidation of Jet A-1 and RME/Jet A-1 mixtures

† Part of the special issue "James A. Miller Festschrift".

* To whom correspondence should be addressed. E-mail: dagaut@cnrs-orleans.fr. Phone: (33) 238 25 54 66. Fax: (33) 238 69 60 04.

10.1021/jp067525j CCC: $37.00
Published on Web 01/25/2007

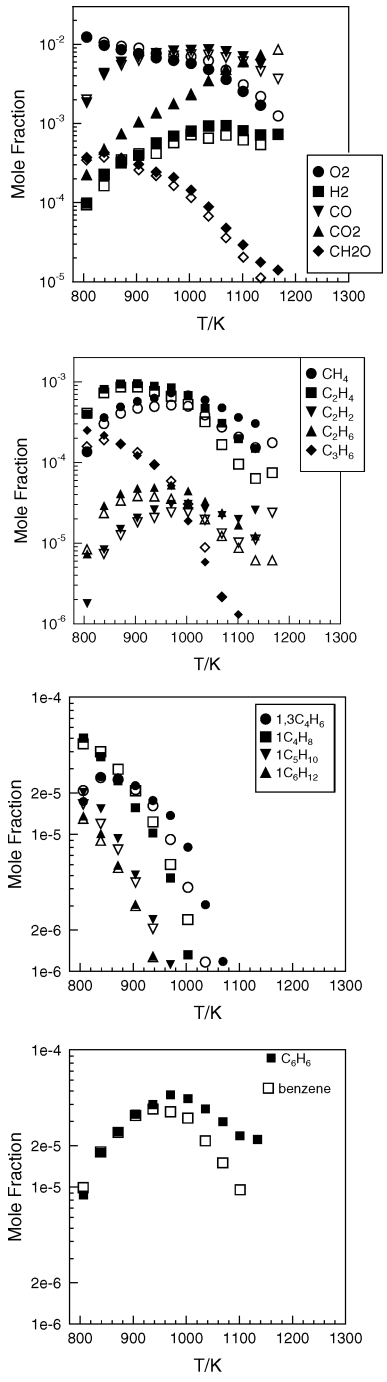

Figure 1. Compared concentration profiles obtained from the oxidation of Jet A-1 (closed symbols) and biokerosene (Jet A-1/RME, 80/20, mol/mol; open symbols) in a JSR (10 atm, $\tau = 0.5$ s, 0.1 mol % Jet A-1, 12384 ppm carbon, $\varphi = 1$).

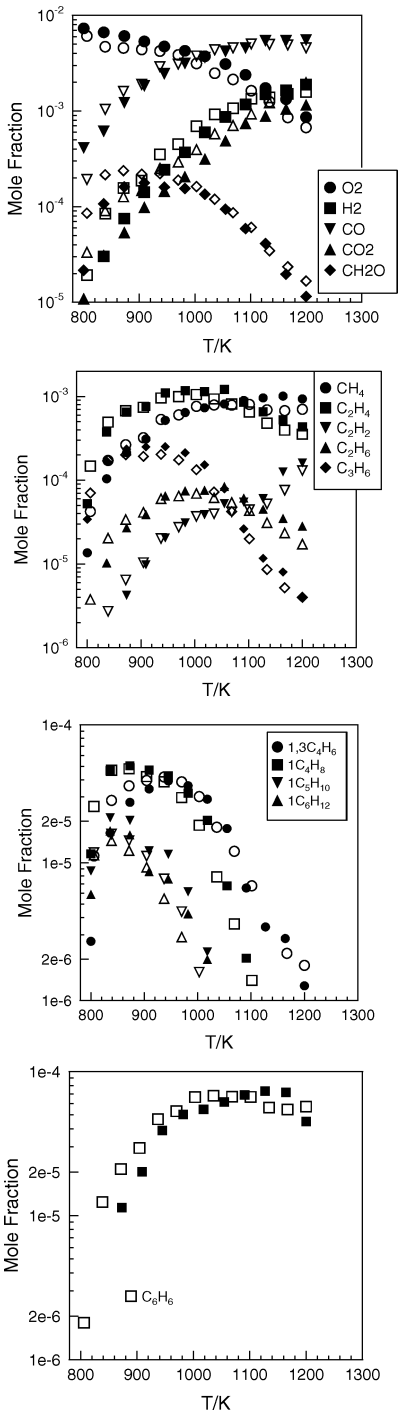

Figure 2. Compared concentration profiles obtained from the oxidation of Jet A-1 (closed symbols) and biokerosene (Jet A-1/RME, 80/20, mol/mol; open symbols) in a JSR (10 atm, $\tau = 0.5$ s, 0.067 mol % Jet A-1, 7370 ppm carbon, $\varphi = 1.5$).

at 10 atm, over a wide range of equivalence ratios ($\varphi = 0.5-1.5$) and temperatures (740−1200 K). The oxidation of kerosene and that of the RME/kerosene blends under JSR, shock-tube, and premixed flame conditions is modeled. The formation of potential soot precursors is also studied.

Experimental Setup

We used the JSR experimental setup described earlier.[15−17,20,23] The JSR consisted of a small sphere of 4 cm diameter (39 cm^3) made of fused silica (to minimize wall catalytic reactions), equipped with four nozzles of 1 mm i.d. for the admission of the gases which achieve stirring. A nitrogen flow of 100 L/h was used to dilute the fuel. As before,[15−17,20,23] all the gases were preheated before injection to minimize temperature gradients inside the reactor. A regulated heating wire of ca. 1.5 kW maintained the temperature of the reactor at the desired working temperature. The reactants were diluted by nitrogen (<50 ppm O_2, <1000 ppm Ar, <5 ppm H_2) and mixed at the entrance of the injectors. High-purity oxygen (99.995% pure) was used in these experiments. Kerosene Jet A-1 and RME were sonically degassed before use. A Shimadzu LC10 AD VP pump with an on-line degasser (Shimadzu DGU-20 A3) was used to deliver the fuel to an atomizer−vaporizer assembly maintained at 200 °C. Good thermal homogeneity along the vertical axis of the reactor was observed for each experiment by thermo-

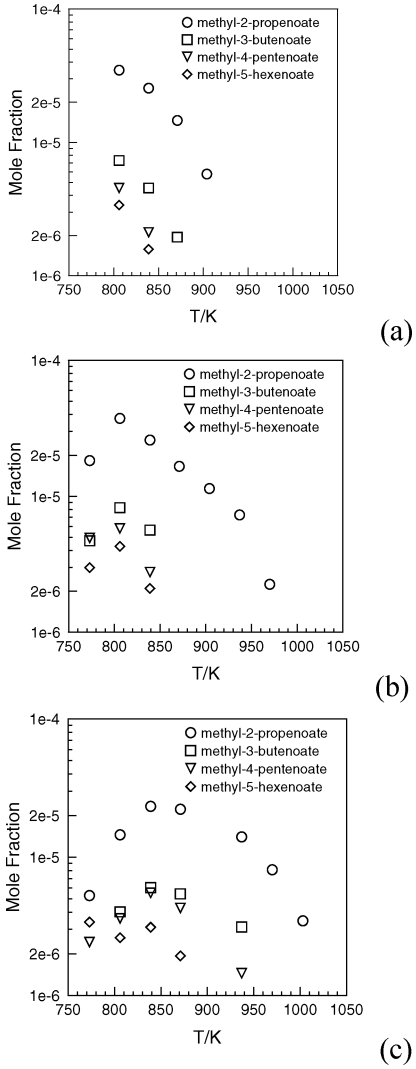

Figure 3. Methyl esters formed from the oxidation of biokerosene (Jet A-1/RME, 80/20, mol/mol) in a JSR at 10 atm, $\tau = 0.5$ s: (a) $\varphi = 0.5$, (b) $\varphi = 1.0$, and (c) $\varphi = 1.5$).

couple (0.1 mm Pt−Pt/Rh (10%) located inside a thin-wall silica tube) measurements (gradients of ca. 1 K/cm). The reacting mixtures were probe sampled by means of a fused silica low-pressure sonic probe. The samples (ca. 4−6 kPa) were taken at steady temperature and residence time. They were analyzed on-line by GC/MS and off-line after collection and storage in 1 L Pyrex bulbs. High-vapor-pressure species and permanent gases were analyzed off-line, whereas low-vapor-pressure compounds were analyzed on-line. The experiments were performed at steady state, at a constant mean residence time, the reactants continually flowing in the reactor, whereas the temperature of the gases inside the JSR was varied stepwise. A high degree of dilution was used, reducing temperature gradients in the JSR and heat release (no flame occurred in the JSR).

Gas chromatographs, equipped with capillary columns (Poraplot-U, Molecular Sieve-5A, DB-5ms, DB-624, Plot Al_2O_3/KCl, Carboplot-P7), a TCD (thermal conductivity detector), and an FID (flame ionization detector) were used for measuring stable species. Compound identifications were made through GC/MS analyses of the samples. A quadrupole mass spectrometer operating in electron impact ionization mode (Varian 1200 GC/MS instrument) was used. As before,[15−17,20,23] CH_2O and CO_2 were measured by the FID after hydrogenation on a Ni/H_2 catalyst connected to the exit of the Poraplot-U GC column. A

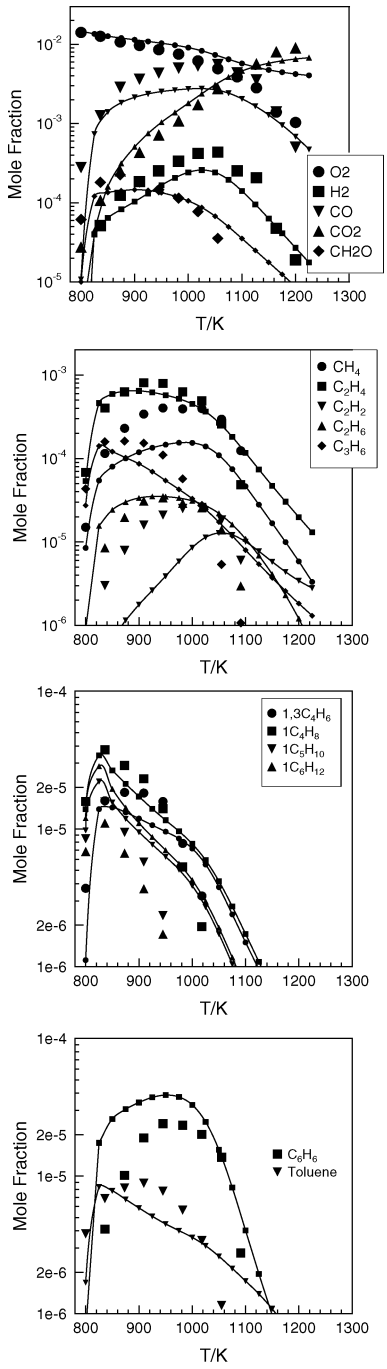

Figure 4. Oxidation of Jet A-1 in a JSR ($\varphi = 0.75$, 10 atm, $\tau = 0.5$ s, 0.067% fuel, 1.474% O_2, total initial carbon concentration of 7370 ppm). The data (large symbols) are compared to the modeling (lines and small symbols).

good repeatability of the measurements and a good carbon balance (100 ± 10%) were obtained in this series of experiments.

The composition of RME was 0.1% C_{14}, 5.4% C_{16}, 92.0% C_{18}, 2.0% C_{20}, and 0.5% C_{22}, with mostly one double bond on the acid chain. The equation for the oxidation of RME can be written as follows: $C_{17.92}H_{33}O_2 + 25.17O_2 \rightleftarrows 17.92CO_2 + 16.5H_2O$.

Modeling

The kinetic modeling was performed using the Chemkin computer package.[24−27] Premixed flames were simulated using the Premix computer code.[24] The ignition delays were simulated by means of the Senkin code,[25] using the constant-volume

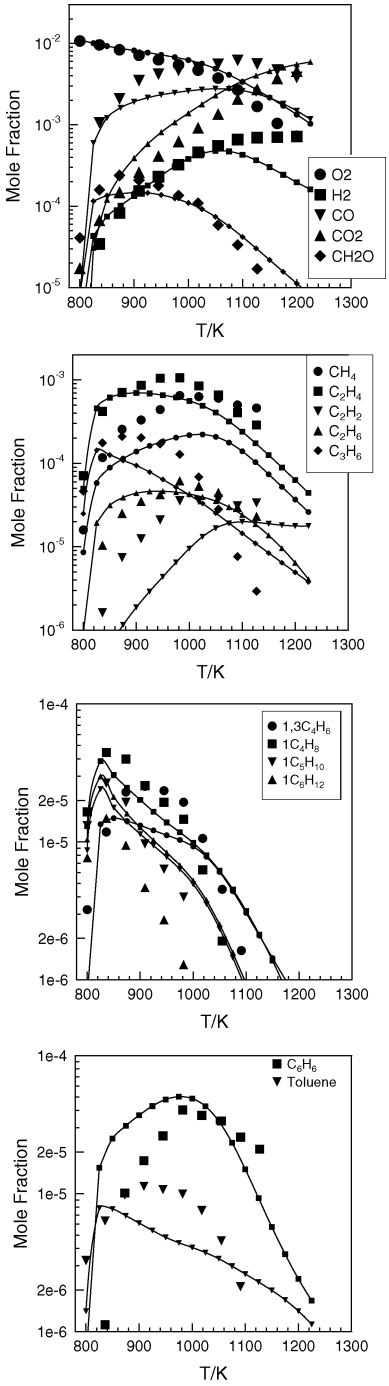

Figure 5. Oxidation of Jet A-1 in a JSR ($\varphi = 1$, 10 atm, $\tau = 0.5$ s, 0.067% fuel, 1.1055% O_2, total initial carbon concentration of 7370 ppm). The data (large symbols) are compared to the modeling (lines and small symbols).

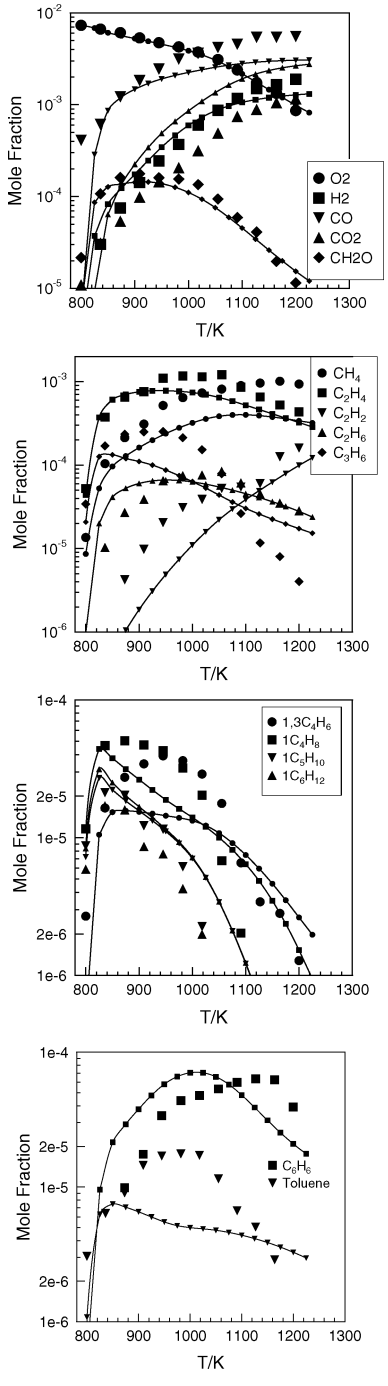

Figure 6. Oxidation of Jet A-1 in a JSR ($\varphi = 1.5$, 10 atm, $\tau = 0.5$ s, 0.067% fuel, 0.737% O_2, total initial carbon concentration of 7370 ppm). The data (large symbols) are compared to the modeling (lines and small symbols).

approximation. For the JSR computations, we used the PSR computer code[26] that computes species concentrations from the balance between the net rate of production of each species by chemical reactions and the difference between the input and output flow rates of the species. These rates are computed from the kinetic reaction mechanism and the rate constants of the elementary reactions calculated at the experimental temperature, using the modified Arrhenius equation $k = AT^b \exp(-E/RT)$. The reaction mechanism used here has a strong hierarchical structure. It is based on the comprehensive kerosene and RME oxidation mechanisms[13,23] developed earlier. The reaction mechanism used here consisted of 263 species and 2027 reversible reactions. This mechanism, including references and thermochemical data, is available from the authors (dagaut@cnrs-orleans.fr). The rate constants for reverse reactions are computed from the corresponding forward rate constants and the appropriate equilibrium constants, $K_c = k_{forward}/k_{reverse}$, calculated from thermochemistry.[27−29]

Results and Discussion

The kinetics of oxidation of RME/kerosene mixtures was studied at 10 atm in a JSR, over the temperature range 740−1200 K, and at a mean residence time of 0.5 s. The experiments were performed at three equivalence ratios, $\varphi = 0.5$, 1, and 1.5. The initial fuel mole fraction was in the range

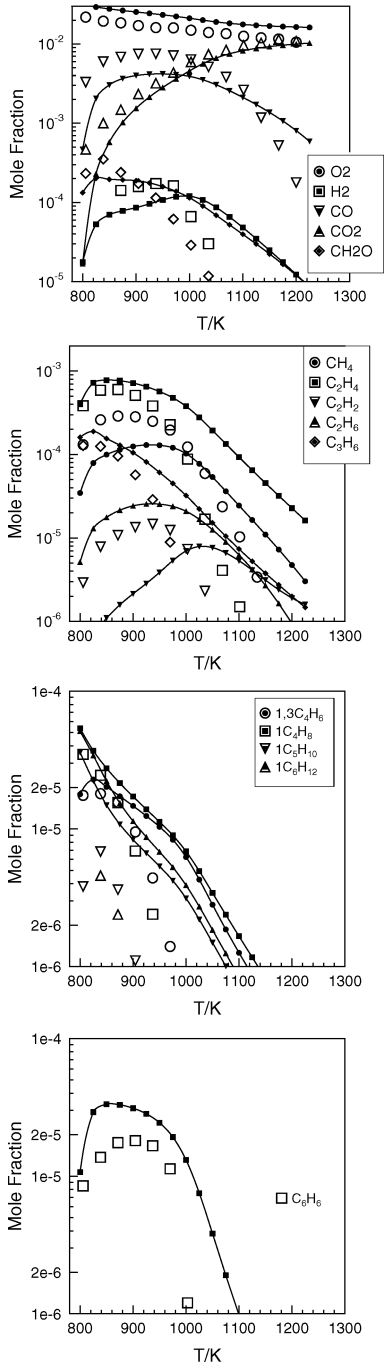

Figure 7. Oxidation of a Jet A-1/RME mixture (80/20, mol/mol) in a JSR ($\varphi = 0.5$, 10 atm, $\tau = 0.5$ s, 806 < *T*/K < 1200, 0.089% fuel, 3.246% O_2, total initial carbon concentration of 11022 ppm). The data (large symbols) are compared to the modeling (lines and small symbols).

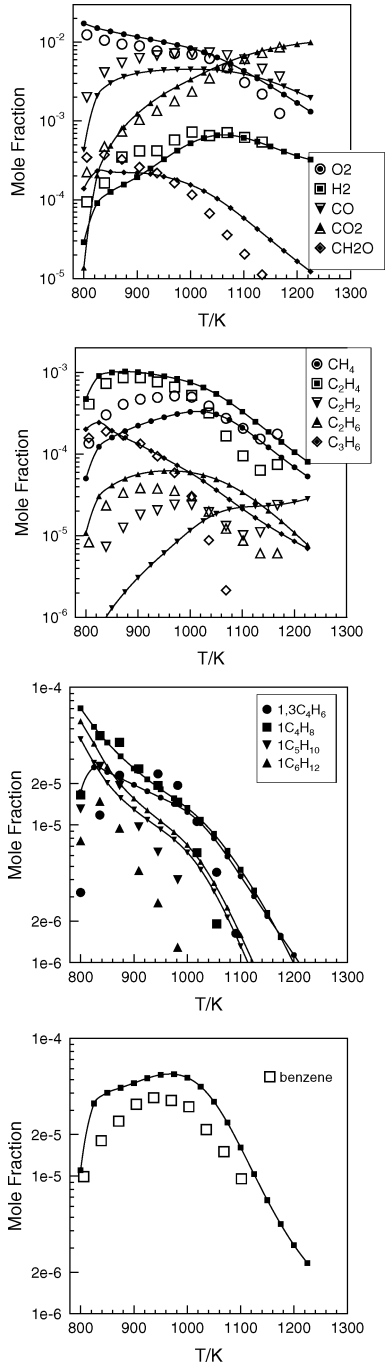

Figure 8. Oxidation of a Jet A-1/RME mixture (80/20, mol/mol) in a JSR ($\varphi = 1$, 10 atm, $\tau = 0.5$ s, 740 < *T*/K < 1200, 0.1% fuel, 1.823% O_2, total initial carbon concentration of 12384 ppm). The data (large symbols) are compared to the modeling (lines and small symbols).

0.0595−0.1. In these conditions, the fuel reacted rapidly, yielding hydrocarbon intermediates (mostly 1-olefins and methane) and oxygenates (mainly formaldehyde and CO). Mole fractions were measured for oxygen, hydrogen, carbon monoxide, carbon dioxide, formaldehyde, methane, ethane, ethene, acetylene, propene, 1-butene, 1-pentene, 1-hexene, 1-heptene, higher alkanes (C_3−C_{10}), methyl esters, and simple aromatics. A good repeatability of the results was observed. The accuracy of the mole fractions was typically ±10% and better than 15%, whereas the uncertainty on the experimental temperature was ±5 K. The comparison of these experimental results with those obtained previously for the oxidation of kerosene[23] in similar conditions indicated a strong similitude. This similitude results from the oxidation of the long saturated alkyl chain present in RME and large *n*-alkanes present in kerosene. However, one should note the reactivity of the RME/kerosene blend is noticeably higher than that of kerosene alone. Nevertheless, the oxidation of the RME/kerosene blend and kerosene produced very similar concentrations of hydrocarbon intermediates. The most noticeable difference between the products of oxidation of the two fuels is the formation of light unsaturated methyl esters deriving from the oxidation of RME. A comparison between the biokerosene blend and kerosene oxidation data is presented in Figures 1 and 2. The main specific products of RME oxidation, consisting of unsaturated methyl esters, are plotted in Figure 3.

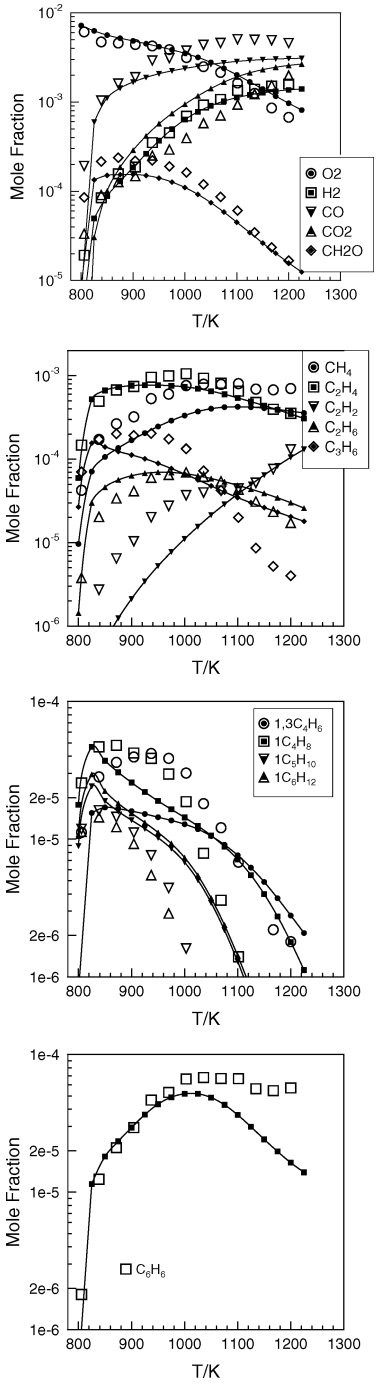

Figure 9. Oxidation of a Jet A-1/RME mixture (80/20, mol/mol) in a JSR (φ = 1.5, 10 atm, τ = 0.5 s, 740 < *T*/K < 1200, 0.0595% fuel, 1.823% O_2, total initial carbon concentration of 7368 ppm). The data (large symbols) are compared to the modeling (lines and small symbols).

This new set of experimental data was used to validate a detailed chemical kinetic reaction mechanism for the oxidation of kerosene/RME blends. First, the oxidation of Jet A-1 was modeled (Figures 4−6). As can be seen from these figures, the agreement between the data and the modeling is similar to that obtained previously.[15,23] In these computations, the jet fuel was represented by a mixture of *n*-decane, *n*-propylbenzene, and *n*-propylcyclohexane (69, 20, and 11 mol %). Since the RME global formula is $C_{17.92}H_{33}O_2$ and that of kerosene is $C_{11}H_{22}$, the resulting global formula for the biokerosene mixture (80 mol % Jet A-1, 20 mol % RME) is $C_{12.384}H_{24.2}O_{0.4}$. The model fuel used here for modeling the kinetics of oxidation of the Jet A-1/RME blend consisted of a mixture of *n*-decane/*n*-propylbenzene/*n*-propylcyclohexane/*n*-hexadecane. The inclusion of *n*-hexadecane in the composition of the present model fuel was motivated by our previous modeling of RME oxidation performed in similar conditions[13] where *n*-hexadecane was used as a model fuel. The model fuel used for modeling the oxidation of the kerosene/RME blend (80/20, mol/mol) was *n*-decane (53.5 mol %), *n*-propylbenzene (17.2 mol %), *n*-propylcyclohexane (9.5 mol %), and *n*-hexadecane (19.8 mol %). Comparisons between experimental and computational results are presented in Figures 7−9. As can be seen from these figures, the proposed model represents reasonably well the kinetics of oxidation of the biokerosene (Jet A-1/RME blend).

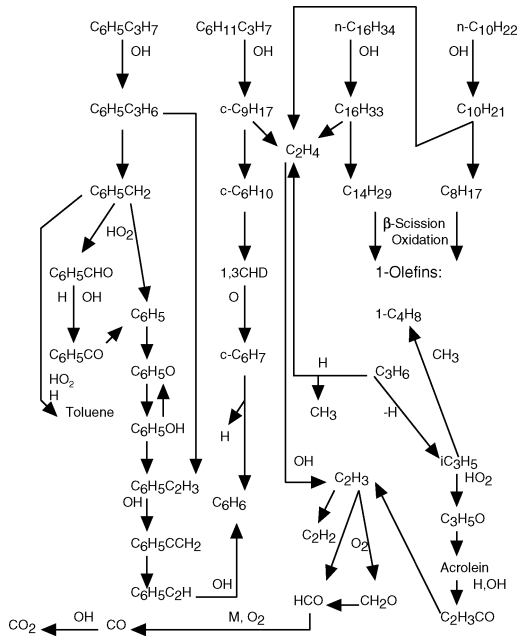

Figure 10. Reaction paths for biokerosene oxidation drawn from the modeling using the selected four-component model fuel.

A kinetic analysis of the reaction paths during the oxidation at 10 atm of the stoichiometric biokerosene mixture (Figure 10) indicates that the overall oxidation of the fuel is driven by *n*-decane. According to the model, at 900 K, in the conditions of Figure 8, hydroxyl radicals are the main species involved in the oxidation of the fuel mixture. The oxidations of *n*-hexadecane and *n*-decane are responsible for the production of these radicals via a complex reaction scheme that can be summarized as follows:

$$n\text{-}C_{16}H_{34} \Rightarrow x\text{-}C_{16}H_{33}\ (x = 1-8)$$

$$n\text{-}C_{10}H_{22} \Rightarrow 3\text{-}C_{10}H_{21},\ 4\text{-}C_{10}H_{21},\ \text{and}\ 5\text{-}C_{10}H_{21}$$

$$n\text{-}C_{10}H_{22} \Rightarrow x\text{-}C_8H_{17}\ (x = 1-4)$$

These alkyl radicals isomerize and decompose. Their decomposition yields ethylene via β-scission and smaller alkyl radicals such as 1-butyl radical that in turn decompose. The further reactions yield OH radicals:

$$1\text{-}C_4H_9 + M \Rightarrow C_2H_5 + C_2H_4 + M$$

$$C_2H_5 + O_2 \Rightarrow C_2H_4 + HO_2$$

$$2HO_2 \Rightarrow H_2O_2 + O_2$$

$$H_2O_2 + M \Rightarrow OH + OH + M$$

$$CH_3 + HO_2 \Rightarrow OH + CH_3O$$

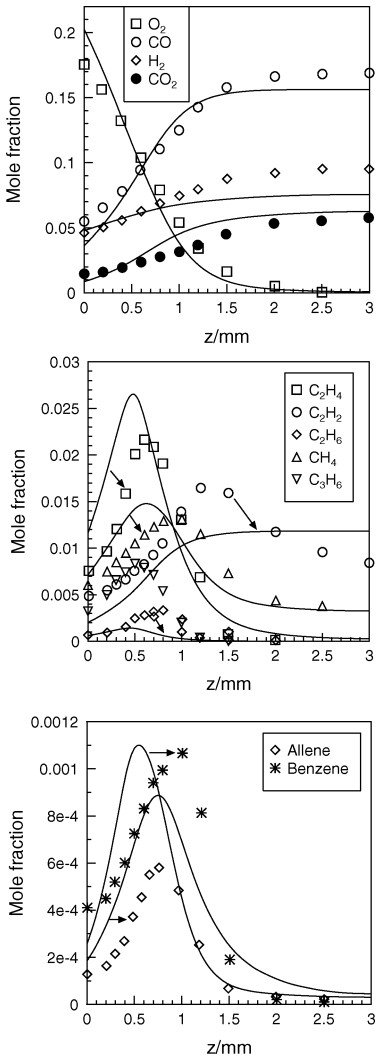

Figure 11. Oxidation of kerosene under premixed flame conditions (1 atm, 0.010739794 (g/cm^2)/s, initial mole fractions 0.0319 of kerosene and 0.28643 of oxygen). The data of ref 9 (symbols) are compared to the modeling (lines). The initial mole fractions used in the modeling were *n*-decane, 0.02463685, *n*-propylbenzene, 0.004993912, *n*-propylcyclohexane, 0.003662271, O_2, 0.28643, and N_2, 0.680276967.

The kerosene premixed flame of Douté et al.[18] studied at atmospheric pressure was also simulated in the present study to further verify the validity of the proposed kinetic model. We used the experimental temperature profile reported by the authors[18] in our computations. As can be seen from Figure 11, the model represents fairly well the experimental concentration profiles of this atmospheric pressure flame. Actually, the computed mole fraction profiles are in very close agreement with those previously computed using an earlier version of the kinetic scheme.[23]

The ignition delays have been simulated before for kerosene/air mixtures,[15,23] demonstrating the accuracy of the kinetic model. Here, we present a comparison of the predicted kerosene/air and biokerosene/air ignition delays for stoichiometric mixtures. For kerosene, the composition of the model fuel was (mole fraction) *n*-$C_{10}H_{22}$, 0.009538353, $C_6H_5C_3H_7$, 0.00276474, $C_6H_{11}C_3H_7$, 0.001520607, O_2, 0.207361, and N_2, 0.7788153. For biokerosene, unfortunately, no ignition data are presently available. In the modeling, the biokerosene composition used was (mole fraction) *n*-$C_{10}H_{22}$, 0.0067779, $C_6H_5C_3H_7$, 0.0021829, $C_6H_{11}C_3H_7$, 0.0012006, *n*-$C_{16}H_{34}$, 0.0025004, O_2, 0.207361, and N_2, 0.7799772. As can be seen from Figure 12, according to the present kinetic model, the ignition delays of biokerosene are undistinguishable from those of Jet A-1. This is an interesting result that should be verified experimentally.

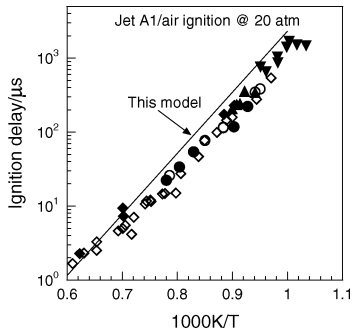

Figure 12. Computed ignition delays of kerosene/air and biokerosene/air mixtures at 20 atm compared to kerosene/air ignition delays in shock tubes. The data were taken from the review paper.[15]

TABLE 1: Computed Maximum Mole Fractions (X_{max}) during the Oxidation of Biokerosene and Jet A-1 in Air in Plug-Flow Conditions (φ = 1, 40 atm, Initial Temperature 800 K)

	biokerosene			Jet A-1			
species	X_{max}	t^a/s	T^b/K	X_{max}	t^a/s	T^b/K	Δ/%
C_2H_4	9.29E−3	0.253	1437	8.44E−3	0.272	1428	10
C_3H_6	1.74E−3	0.253	1372	1.67E−3	0.272	1370	4.2
C_2H_2	1.66E−3	0.253	1824	1.63E−3	0.272	1809	1.8
C_6H_6	5.58E−4	0.253	1084	6.62E−4	0.271	1032	−15.7
pC_3H_4	3.50E−4	0.253	1647	3.32E−4	0.272	1662	5.4
1,3-C_4H_6	6.07E−4	0.253	1368	6.24E−4	0.272	1115	−2.7
$C_{10}H_8$	1.15E−6	0.253	2466	1.71E−6	0.272	2476	−32.7

[a] Residence time where the maximum mole fraction is computed. [b] Temperature where the maximum mole fraction is computed.

TABLE 2: Computed Maximum Mole Fractions (X_{max}) during the Oxidation of Biokerosene and Jet A-1 in Air in Plug-Flow Conditions (φ = 1.5, 40 atm, Initial Temperature 800 K)

	biokerosene			Jet A-1			
species	X_{max}	t^a/s	T^b/K	X_{max}	t^a/s	T^b/K	Δ/%
C_2H_4	1.06E−2	0.285	1373	9.72E−3	0.303	1428	9.1
C_3H_6	2.11E−3	0.285	1377	2.03E−3	0.303	1322	3.9
C_2H_2	3.53E−3	0.285	1901	3.16E−3	0.303	1868	11.4
C_6H_6	7.06E−4	0.285	1323	8.30E−4	0.303	1316	−14.9
pC_3H_4	3.91E−4	0.285	1487	3.69E−4	0.303	1483	5.9
1,3-C_4H_6	7.05E−4	0.285	1333	7.29E−4	0.303	1324	−3.3
$C_{10}H_8$	4.95E−6	0.285	1813	7.06E−6	0.303	19206	−29.8

[a] Residence time where the maximum mole fraction is computed. [b] Temperature where the maximum mole fraction is computed.

Using the present kinetic model, we investigated the effect of changing the fuel composition on the formation of potential PAH or soot precursors (Tables 1 and 2). These tables indicate consistency in the simulation for stoichiometric and fuel-rich conditions. The model correctly predicts that, in the case of biokerosene combustion, since the initial fraction of aromatics is less than in Jet A-1 (−21%), less aromatic hydrocarbons are produced. The computed maximum mole fraction of benzene is reduced by ca. 15% and that of naphthalene ($C_{10}H_8$) by ca. 30%. Also, the fraction of 1,3-butadiene is reduced in the biokerosene combustion case. This result must also be attributed to the reduction in the initial mole fraction of aromatics (−21%) and cycloalkanes (−21%), which is balanced by the production

of butadiene through the oxidation of *n*-hexadecane. The model predicts the oxidation of the biokerosene yields more ethylene, acetylene, propene, and propyne than Jet A-1. This is actually the result of the mechanism presented above through which the long alkane chain of *n*-hexadecane yields small 1-olefins (mostly ethylene and propene) by β-scission. The further reactions of ethylene yield acetylene via the intermediate formation of the vinyl radical. The oxidation of propene is an important source of propyne through the intermediate formation of the allyl radical. A comparison of these computed trends with the present data shows several discrepancies that should be addressed in future modeling. The increased production of 1-olefins from the oxidation of the biokerosene was not observed experimentally, which can be attributed to the fact the long hydrocarbon chain in the esters is partially unsaturated, resulting in less 1-olefin production than from *n*-hexadecane oxidation. The model and the data agree on the reduced production of benzene from the oxidation of the biokerosene (ca. −28% in the stoichiometric case). Since naphthalene is present in Jet A-1, it was not possible to study experimentally the impact of the fuel reformulation on this PAH.

In a recent paper on reformulated diesel combustion,[30] the authors showed the strong impact of several of the oxygenates they considered. However, their results indicated the use of a long-chain ester has a moderate effect on soot production (reduction of ca. 27% of the Bosch index). The inclusion of 20% $C_{17.92}H_{33}O_2$ is not expected to strongly affect the fuel oxidation chemistry as would multioxygenated structures since methyl ester radicals undergo bond scission, preferentially yielding CO_2,[31,32] which does not remove soot precursors.

Conclusion

The oxidation of kerosene Jet A-1 and a biokerosene blend (Jet A-1/RME, 80/20, mol/mol) was studied experimentally in a jet-stirred reactor at 10 atm and constant residence time, over the temperature range 740−1200 K, and for variable equivalence ratios in the range 0.5−1.5. Concentration profiles of reactants, stable intermediates, and final products were obtained by probe sampling followed by on-line and off-line GC analyses. No significant variation of the concentration of the products was observed by changing the fuel from Jet A-1 to biokerosene besides the formation of monounsaturated methyl esters (<50 ppm) produced from the oxidation of RME. These experiments were simulated using a detailed chemical kinetic reaction mechanism consisting of 2027 reversible reactions and 263 species. The surrogate biokerosene model fuel used consisted of a mixture of *n*-hexadecane, *n*-propylcyclohexane, *n*-propylbenzene, and *n*-decane, where the methyl ester fraction was represented by *n*-hexadecane. The proposed chemical kinetic reaction mechanism used in the modeling yielded a reasonably good representation of the kinetics of oxidation of kerosene and biokerosene under JSR conditions. The data and the model showed the RME/Jet A-1 mixture has a slightly higher reactivity than Jet A-1. The ignition of Jet A-1 and that of biokerosene were simulated. The kinetic model does not predict a significant effect of RME on the ignition of kerosene. Therefore, it seems that switching from kerosene to biokerosene (<20% RME) has no major impact on the kinetics of oxidation of the fuel, which is an interesting result allowing the use of relatively simple kinetic schemes for simulating biokerosene oxidation. The formation of potential soot precursors was studied using the proposed kinetic scheme. It showed some discrepancies between the data and the modeling, mostly attributed to the use of a saturated long-chain hydrocarbon to represent RME, rather than an unsaturated chemical, yielding more 1-olefins than the unsaturated methyl esters.

Supporting Information Available: Table of thermodynamic data. This material is available free of charge via the Internet at http://pubs.acs.org.

References and Notes

(1) Shauck, M. E.; Zanin, G.; Alvarez, S. 9th International Conference on Stability, Handling and Use of Liquid Fuels, Sitges, Spain, Sept 18−22, 2005.

(2) Delafontaine, M.; Dunn, R. O.; Hubert, M.; Krishna, C. R. 9th International Conference on Stability, Handling and Use of Liquid Fuels, Sitges, Spain, Sept 18−22, 2005.

(3) Daggett, D.; Hadaller, O.; Hendricks, R.; Walther, R. 25th International Congress of the Aeronautical Sciences, Hamburg, Germany, Sept 3−8, 2006.

(4) Ryan, L.; Convery, F.; Ferreira, S. *Energy Policy* **2006**, *34*, 3184−3194.

(5) U.S. Environmental Protection Agency. *A comprehensive analysis of biodiesel impacts on exhaust emissions*; Report EPA420-P-02-001; Washington, DC, October 2002.

(6) Garrett, T. K. *Automotive fuels and fuel systems. Vol. 2: Diesel*; Pentech Press: London, 1994.

(7) Sheehan, J.; Camobreco, V.; Duffield, J.; Graboski, M.; Shapouri, H. *Life cycle inventory of biodiesel and petroleum diesel for use in an urban bus*; National Renewable Energy Laboratory Report NREL/SR-580-24089; Washington, DC, May 1998.

(8) Schröder, O.; Frahl, J.; Munack, A.; Krahl, J.; Bünger, J. SAE 1999-01-3561; Society of Automotive Engineers: Warrendale, PA, 1999.

(9) Montagne, X. SAE 962065; Society of Automotive Engineers: Warrendale, Pa, 1996; pp 247−256.

(10) Krahl, J.; Munack, A.; Bahadir, M.; Schumacher, L.; Elser, N. SAE 962096; Society of Automotive Engineers: Warrendale, PA, 1996; pp 319−338.

(11) Graboski, M. S.; McCormick, R. L. *Prog. Energy Combust. Sci.* **1998**, *24*, 125−164.

(12) Ramadhas, A. S.; Jayaraj, S.; Muraleedharan, C. *Renewable Energy* **2004**, *29*, 727−742.

(13) Dagaut, P.; Gaïl, S.; Sahasrabudhe, M. *Proc. Combust. Inst.* **2007**, *31*, 2955−2961.

(14) Jeuland, N.; Montagne, X.; Duret, P. *Oil Gas Sci. Technol.—Rev. IFP* **2004**, *6*, 571−579.

(15) Dagaut, P.; Cathonnet, M. *Prog. Energy Combust. Sci.* **2006**, *32*, 48−92.

(16) Dagaut, P.; Reuillon, M.; Boettner, J.-C.; Cathonnet, M. *Proc. Combust. Inst.* **1994**, *25*, 919−926.

(17) Dagaut, P.; Reuillon, M.; Cathonnet, M.; Voisin, D. *J. Chim. Phys. Phys.-Chim. Biol.* **1995**, *92*, 47−76.

(18) Douté, C.; Delfau, J.-L.; Akrich, R.; Vovelle, C. *Combust. Sci. Technol.* **1995**, *106*, 327−344.

(19) Mawid, M. A.; Park, T. W.; Sekar, B.; Arana, C. *38th Joint Propulsion Conference and Exhibit*, Indianapolis, IN, July 7−10, 2002; AIAA 2002-3876; American Institute of Aeronautics and Astronautics: Reston, VA, 2002.

(20) Dagaut, P. *Phys. Chem. Chem. Phys.* **2002**, *4*, 2079−2094.

(21) Mawid, M. A.; Park, T. W.; Sekar, B.; Arana, C. *39th Joint Propulsion Conference and Exhibit*, Huntsville, AL, July 20−23, 2003; AIAA 2003-4938; American Institute of Aeronautics and Astronautics: Reston, VA, 2003.

(22) Mawid, M. A.; Park, T. W.; Sekar, B.; Arana, C. *40th Joint Propulsion Conference and Exhibit*, Fort Lauderdale, FL, July 11−14, 2004; AIAA 2004-4207; American Institute of Aeronautics and Astronautics: Reston, VA, 2004.

(23) Dagaut, P. *Proceedings of ASME Turbo Expo 2006: Power for Land, Sea, and Air*, Barcelona, Spain, May 8−11, 2006; American Society of Mechanical Engineers: New York, 2006.

(24) Kee, R. J.; Grcar, J. F.; Smooke, M. D.; Miller, J. A. *Premix: A Fortran program for modeling steady laminar one-dimensional premixed flame*; Sandia Report No. SAND85-8240; Sandia National Laboratories: Livermore, CA, 1985.

(25) Lutz, A. E.; Kee, R. J.; Miller, J. A. *Senkin: A Fortran program for predicting homogeneous gas phase chemical kinetics with sensitivity analysis*; Sandia Report No. SAND87-8248; Sandia National Laboratories: Livermore, CA, 1988.

(26) Glarborg, P.; Kee, R. J.; Grcar, J. F.; Miller, J. A. *PSR: A FORTRAN program for modeling well-stirred reactors*; Sandia Report No. SAND86-8209, Sandia National Laboratories: Livermore, CA, 1986.

(27) Kee, R. J.; Rupley, F. M.; Miller, J. A. *Thermodynamic data base*; Sandia Report SAND87-8215; Sandia National Laboratories: Livermore, CA, 1991.

(28) Tan, Y.; Dagaut, P.; Cathonnet, M.; Boettner, J.-C. *Combust. Sci. Technol.* **1994**, *102*, 21−55.

(29) Muller, C.; Michel, V.; Scacchi, G.; Côme, G.-M. *J. Chim. Phys. Phys.-Chim. Biol.* **1995**, *92*, 1154−1178.

(30) Miyamoto, N.; Ogawa, H.; Nurun, N. M.; Obata, K.; Arima, T. SAE 980506; Society of Automotive Engineers: Warrendale, PA, 1998.

(31) McCunn, L. R.; Lau, K.-C.; Krisch, M. J.; Butler, L. J.; Tsung, J.-W.; Lin, J. J. *J. Phys. Chem. A* **2006**, *110*, 1625−1634.

(32) Westbrook, C. K.; Pitz, W. J.; Curran, H. J. *J. Phys. Chem. A* **2006**, *110*, 6912−6922.